

# Study on Morphology Behavior of PVDF-Based Electrolytes

Li-ying Tian, Xiao-bin Huang, Xiao-zhen Tang

School of Chemistry and Chemical Technology, Shanghai Jiaotong University, Shanghai 200240, China

Received 26 June 2003; accepted 2 December 2003

**ABSTRACT:** Three nonelectrolyte samples and one gel polymer electrolyte sample were prepared from poly(vinylidene fluoride) (PVDF), propylene glycol carbonate (PC), and  $\text{LiClO}_4$  in the present article. Fourier transform infrared spectroscopy, dynamic mechanical analysis, differential scanning calorimetry, thermogravimetric analysis, X-ray diffraction, and scanning electron microscopy were used to study morphology structure of all the samples. Results showed that there were great interactions among PVDF, PC,

and lithium salt, which led to different morphology properties of different samples. Interactions between PVDF and PC mainly occurred on the surface area of PVDF crystalline, while interactions between PC, PVDF, and lithium salt mainly occurred in the amorphous area. © 2004 Wiley Periodicals, Inc. *J Appl Polym Sci* 92: 3839–3842, 2004

**Key words:** structure–property relations; morphology; dynamic mechanical analysis; gel polymer electrolyte

## INTRODUCTION

With good thermal, mechanical, and electrochemical stability, fluorine-containing polymer materials, such as poly(vinylidene fluoride) (PVDF)<sup>1,2</sup> and modified PVDF,<sup>3,4,5</sup> were more suitable than polymethylmethacrylate (PMMA) and polyacrylonitrile (PAN) when used as polymer host in gel polymer electrolytes (GPEs). However, most of the relevant research focused attention on ionic conductive property of electrolyte material and charge–discharge behavior of lithium batteries. Regarding morphology property and ionic conductive mechanism of gel polymer electrolytes based on PVDF, there were still many aspects that needed further investigating.

In the present article, three nonelectrolyte samples and one GPE sample were prepared from PVDF, PC, and lithium salt ( $\text{LiClO}_4$ ) by the solvent-casting technique. Morphology properties of all the samples were studied in detail by Fourier transform infrared spectroscopy (FTIR), dynamic mechanical analysis (DMA), differential scanning calorimetry (DSC), thermogravimetric analysis (TGA), X-ray diffraction (WAXD), and scanning electron microscopy (SEM).

## EXPERIMENTAL

### Chemicals

PVDF (FR921) was supplied by Shanghai 3F New Material Co. Ltd. (China). Propylene glycol carbonate

(PC), *N,N*-dimethylformamide (DMF, chemically pure grade, Shanghai Chemical Factory, China) and lithium perchlorate ( $\text{LiClO}_4$ ), analytical reagent grade (Shanghai No. 2 Chemical Factory, China) were used as received.

### Preparation of samples

All samples were prepared by the solvent-casting technique. PVDF, PC, and  $\text{LiClO}_4$  were dissolved in DMF, and then the solutions were cast into an aluminum plate. Film formed in an oven under vacuum at 60°C. Compositions of the samples were shown in their symbols, for example, PVDF/PC = 1.5/1.0 meant that the weight ratio of PVDF/PC was 1.5/1.0; similarly, PVDF/PC/ $\text{LiClO}_4$  = 1.5/1.0/0.4 meant the weight ratio of PVDF/PC/ $\text{LiClO}_4$  was 1.5/1.0/0.4.

### Characterization

Infrared spectra (IR) were recorded on a Perkin–Elmer 963 FTIR analyzer. The dynamic mechanical analysis was carried out on a Rheometric Scientific DMTA-IV type apparatus. Frequencies chosen were 1 Hz and the temperature range was between –100 and 100°C with an increase rate of 5°C/min. DSC scans were carried out on a Perkin–Elmer Pyris-1 differential scanning calorimetry in a temperature range of 20–200°C with a temperature increase rate of 20°C/min, and nitrogen of 20 mL/min was used. The thermal stability of the samples was investigated by using a thermogravimetric analyzer (model TGA 7, Perkin–Elmer) in nitrogen flow. The heating rate was 20°C/min. WAXD patterns of PVDF and the electrolyte were obtained by means

Correspondence to: X.-Z. Tang (Xtang@mail.sjtu.edu.cn).

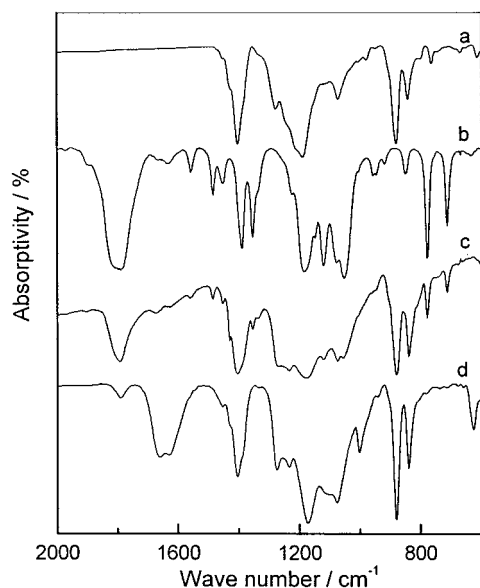


**Figure 1** Infrared spectra of PVDF, PC, PVDF/PC, and electrolyte sample.

of Bruker-AXS D8 advance diffractometer by using Cu-K $\alpha$  radiation. SEM was carried out on a Hitachi S2150 scanning electron microscope, and the surface of the samples was analyzed.

## RESULTS AND DISCUSSION

### Infrared spectra analysis

Infrared spectra of PVDF, PC, PVDF/PC, and the electrolyte sample were shown in Figure 1. For the spectra of the samples, a peak of about 1800  $\text{cm}^{-1}$  was attributed to free carbonyl of PC, whereas a peak of about 1650  $\text{cm}^{-1}$  was attributed to bonded carbonyl of PC.<sup>6</sup> It could be found that, in the spectrum of PVDF/PC, the peak of about 1650  $\text{cm}^{-1}$  was more evident than that of PC, which suggested that more carbonyl of PC was bonded and this should be attributed to the interaction between PC and PVDF. For the gel electrolyte sample, the peak at about 1800  $\text{cm}^{-1}$  had almost disappeared and the peak of bonded carbonyl of about 1650  $\text{cm}^{-1}$  became stronger, which meant a complex interaction happened between lithium ion and carbonyl of PC.

### Dynamic mechanical analysis

The dynamic mechanical relaxation spectrum of PVDF, which had been widely studied,<sup>7,8</sup> presented four different relaxations [Fig. 2(a)].  $\alpha$ -Relaxation (about 100°C) belonged to the crystalline phase.  $\beta'$ -Relaxation (about 25°C) appeared in the amorphous phases and was attributed to the fold-chain segment of PVDF on the surface of crystalline phase.  $\beta$ -Relaxation

(-40°C) corresponded to glass transition and hence to Brownian micromotion in the backbone in the amorphous zones. Finally,  $\gamma$ -relaxation (-75°C) was attributed to restricted motion of about several carbon atoms in the amorphous phase.

From Figure 2(b), it could also be found that, with additive of PC into PVDF, the  $\beta'$ -transition enhanced obviously and almost overlaid other transition signals, and the peak of  $\beta'$ -transition moved toward low temperature. This result suggested that the effect of PC was mostly on the surface of the crystalline phase of PVDF, and the additive of PC led to the collapse of some crystalline of PVDF, which resulted in expansion of the surface area of PVDF crystalline.

The affiliation of LiClO<sub>4</sub> had evident influence on both  $\beta'$ - and  $\beta$ -transition [in Fig. 2(c)], and the position of these two transitional peaks all moved to a lower temperature.  $\beta$ -Transition enhanced obviously compared to other transitions, which meant LiClO<sub>4</sub> had several effects on PVDF as follows: (1) LiClO<sub>4</sub> had a great effect on the PVDF in noncrystalline region, which was the main effect of LiClO<sub>4</sub> on PVDF; (2) at the same time, LiClO<sub>4</sub> also had some effect on the surface of crystalline PVDF, which led to collapse of some PVDF crystalline, and then resulted in an increase of the ratio of amorphous zone.

For the curve of Figure 2(d), which was similar to that of Figure 2(c), the position of  $\beta$ -transitions peaks moved to a temperature region lower than those of other curves, which suggested that the interactions among PC, LiClO<sub>4</sub>, and PVDF mostly occurred in the noncrystalline region, and PC acted as a kind of plasticizer in the matrix of PVDF/PC/LiClO<sub>4</sub>.

### DSC analysis

DSC plots for PVDF, PVDF/LiClO<sub>4</sub>, PVDF/PC, and PVDF/PC/LiClO<sub>4</sub> in the temperature range of 20–200°C were shown in Figure 3. In the DSC curves of PVDF and PVDF/LiClO<sub>4</sub>, there were endothermic peaks at about 160°C, which were attributed to the

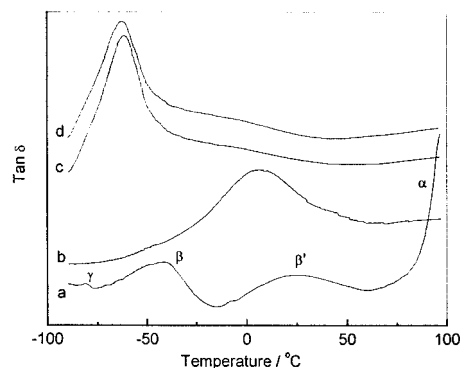


**Figure 2** DMA curves of different PVDF samples (1 Hz).

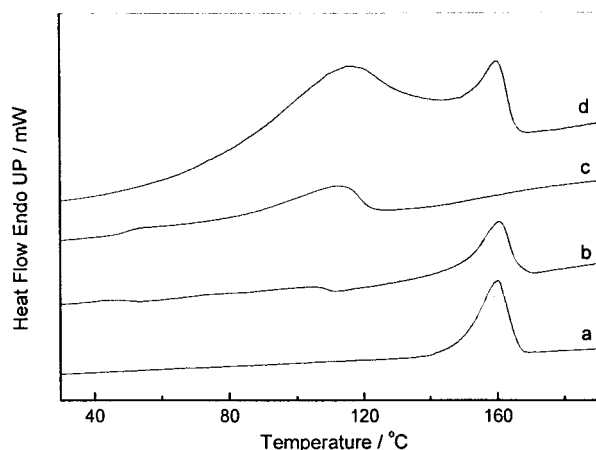


**Figure 3** DSC curves of PVDF, PVDF/LiClO<sub>4</sub>, and PVDF/PC.

melting point of PVDF.<sup>9</sup> While in the DSC curve of PVDF/PC, a broad and weak peak at about 115°C could be found, which might be attributed to another morphologic structure different from pure PVDF. In fact, infrared spectra analysis of PVDF/PC had suggested that there were interactions between PVDF and PC. So, the endothermic peak at about 115°C should be attributed to the morphologic structure of PVDF containing PC. From curves of PVDF/PC = 1.5/1.0 and PVDF/PC/LiClO<sub>4</sub> = 1.5/1.0/0.4, it could be found that, because of the great interaction between lithium ion and PC, when LiClO<sub>4</sub> was added into the matrix, LiClO<sub>4</sub> entered into the phase of PVDF/PC and led to microphase separation, which resulted in two DSC peaks: the peak at about 115°C should be attributed to the phase of PVDF/PC/LiClO<sub>4</sub>, whereas the peak at about 160°C belonged to the phase of pure PVDF formed again.

### TGA analysis

TGA results of PVDF, PVDF/PC, and PVDF/PC/LiClO<sub>4</sub> were shown in Figure 4. There was only one weight-loss peak at 490°C in the curve of PVDF, which was attributed to the decomposition of PVDF. For the sample of PVDF/PC, with the additive of PC, the crystalline of PVDF was broken down to some certain degree and a new microphase structure of PVDF/PC formed, which resulted in three peaks, as shown in the TGA curve of PVDF/PC, and the peaks of 350 and 370°C belonged to the microphase structure of PVDF/PC, while the other peak of 490°C should belong to PVDF.

Compared to PVDF/PC, in the TGA curve of PVDF/PC/LiClO<sub>4</sub>, the two weight-loss peaks at low temperature moved to the high region of temperature (with peak values of 359 and 381°C), and the peak at high-temperature region moved toward the low-temperature region

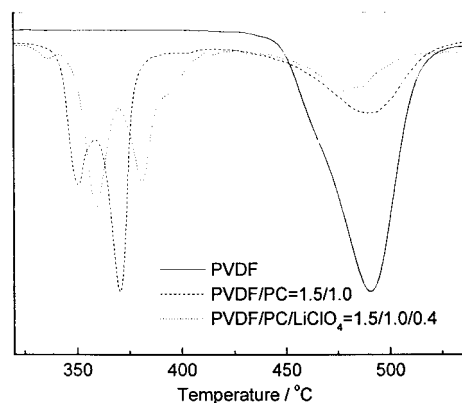


**Figure 4** TGA curves of different PVDF samples.

(the peak value was 480°C). These changes suggested that the microphase structure of PVDF/PC/LiClO<sub>4</sub> was different from that of PVDF/PC.

### WAXD analysis

Figure 5 showed XRD patterns of pure PVDF powder, pure PVDF film, and PVDF/PC/LiClO<sub>4</sub> = 1.5/1.0/0.4, respectively. Both pure PVDF samples (a, b) were characterized by relatively sharp diffraction peaks at  $2\theta = 18.4^\circ$  and  $20^\circ$ , as well as broad peaks centered at  $2\theta = 26.7^\circ$  and  $36^\circ$ .<sup>10</sup> This result elucidated that preparation procedure of the samples had little effect on morphology of PVDF. The X-ray diffraction pattern shown in Figure 5(c) revealed clearly that the gel polymer electrolyte was generally amorphous and its crystallinity was depressed greatly by the addition of PC and LiClO<sub>4</sub>.

### SEM analysis

SEM photographs of PVDF, PVDF/LiClO<sub>4</sub>, PVDF/PC, and PVDF/PC/LiClO<sub>4</sub> are listed in Figure 6. From the pictures, it could be found clearly that the surface

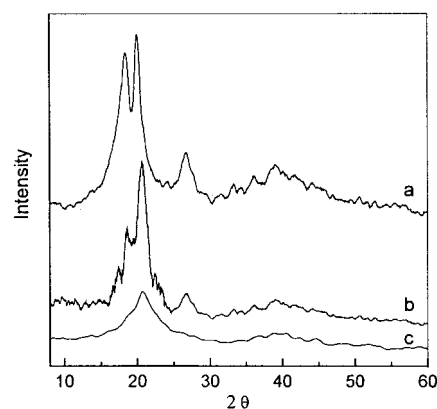


**Figure 5** WAXD spectra of different PVDF samples.

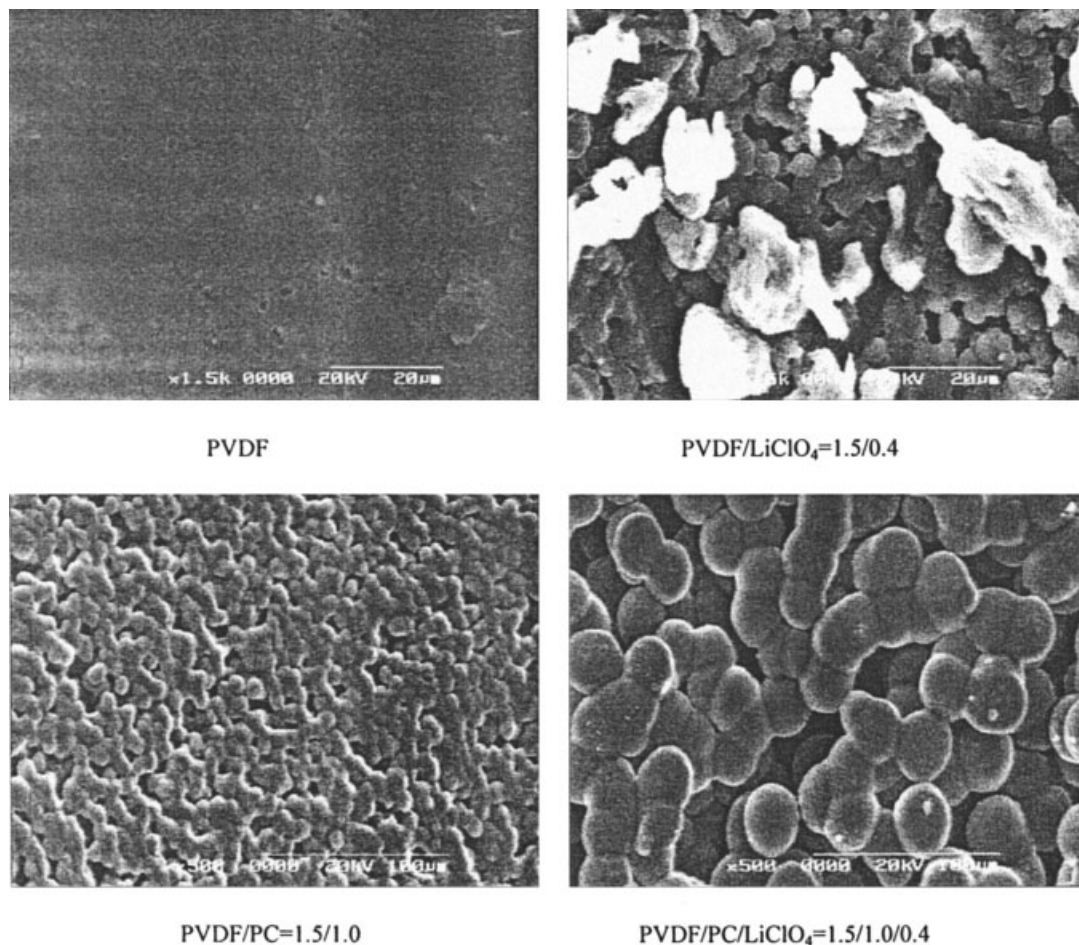


Figure 6 SEM photos of different PVDF samples.

of PVDF was smooth, whereas in the photograph of PVDF/LiClO<sub>4</sub>, evident aggregations attributed to LiClO<sub>4</sub> could be found, which meant that the lithium salt could not be completely dissolved by the PVDF host. For the sample of PVDF/PC, there were many small spherical aggregations, which should be attributed to the PVDF/PC-rich morphologic structure. Results of DSC analysis had suggested that, when lithium salt was added into PVDF/PC, morphology structure of the sample matrix would change from PVDF/PC phase to the phases of both pure PVDF and PVDF/PC/LiClO<sub>4</sub>, and as shown in Figure 6(c, d), such a change of morphology structure caused by lithium salt was evident.

### CONCLUSION

Results showed that there were great interactions among PVDF, PC, and lithium salt, which led to different morphology properties of different samples: in PVDF, there were both a crystalline part and an amorphous zone; in PVDF/PC, morphologic structure of PVDF containing PC was evident; in PVDF/PC/

LiClO<sub>4</sub>, morphology structure changed into phases containing PVDF/PC/LiClO<sub>4</sub>, and a small part of pure PVDF crystalline formed again at the same time. Results also showed that interactions between PVDF and PC mainly happened in the surface area of PVDF crystalline, whereas interactions between PC, PVDF, and lithium salt mainly occurred in amorphous area.

### References

1. Periasamy, P.; Tatsumi, K.; Shikano, M. *J Power Sources* 2000, 88, 269.
2. Yuria, S.; Capiglia, C.; Kataoka, H. *Solid State Ionics* 2000, 136–137, 1161.
3. Capiglia, C.; Saito, Y.; Kataoka, H. *Solid State Ionics* 2000, 131, 291.
4. Chi, S. K.; Oh, M. *Seung Electrochim Acta* 2001, 46, 1323.
5. Arcella, V.; Sanguineti, A.; Quartarone, E. *J Power Sources* 1999, 81–82, 790.
6. Zhu, W. H.; Yang, B.; Tang, X. Z. *J Polym Sci, Part B: Polym Phys* 2001, 39, 1246.
7. Linares, A.; Acosta, J. L. *Eur Polym Mater* 1997, 33, 467.
8. Lovinger, A. J. In *Developments in Crystalline Polymers*; Basset, D. C., Ed.; Applied Science Publishers: London, 1982; Chapter 1.
9. Tazaki, M.; Wada, R.; Okabe, M. *J Appl Polym Sci* 1997, 65, 1517.
10. Jiang, Z.; Carroll, B.; Abranam, K. M. *Electrochim Acta* 1997, 42, 2667.